

SPACE CHARGE COMPENSATED ION BEAM EXTRACTION

J. Rausch^{*,1}, O. Meusel¹, H. Podlech^{1,2,3}

¹Goethe University Frankfurt, Frankfurt, Germany

²Helmholtz Research Academy Hesse for FAIR (HFHF), Frankfurt, Germany

³GSI Helmholtz Centre for Heavy Ion Research, Darmstadt, Germany

Abstract

The generation of high intensity ion beams requires high density plasma in the ion source. Earlier studies [1] have shown how high plasma densities can be achieved with a combined RF- and arc-discharge without using a filament as an electron emitter. While space charge compensation in the extraction region could benefit the space charge limited extraction of high intensity beam, in conventional extraction systems however the compensating electrons need to be blocked from entering the extraction region by means of a suppression voltage to prevent sparking in the high voltage gap. Therefore we propose the controlled use of a separately produced electron beam to compensate space charge right at the extraction gap. The concept of achieving superposition of electron and ion beam by propagating the e- beam through the plasma generator chamber is evaluated. First beam dynamics simulations for the electron beam as well as extraction studies for the compensated and non-compensated case are presented.

INTRODUCTION

Development of Accelerators in recent years is directed more and more towards reaching higher intensities [2–4]. To reach higher beam intensity, first the necessary beam current has to be provided by an ion source. Previous studies have investigated the concept of a hybrid ion source to reach high density plasma states needed for high current beam extraction. This work focuses on the extraction region, where the ion beam is formed by de-neutralizing the plasma and accelerating the ions in a high potential difference in the extraction gap. We propose a method to overcome the limitations of extracted current density given by the Child-Langmuir law by the use of a spacecharge compensating electron beam. While other work [5] has shown partially beneficial effects using a pulsed electron beam, moving upstream towards the ion source and dumped inside the ion source, we investigate the comoving beam which can be created and dumped independently of the ion source. Simulations of the overlapped beams in the triode extraction are performed to show the possibilities for mitigating the space charge limitations.

MOTIVATION

A measure for the maximum current density J that can be extracted using a potential difference across a gap of two

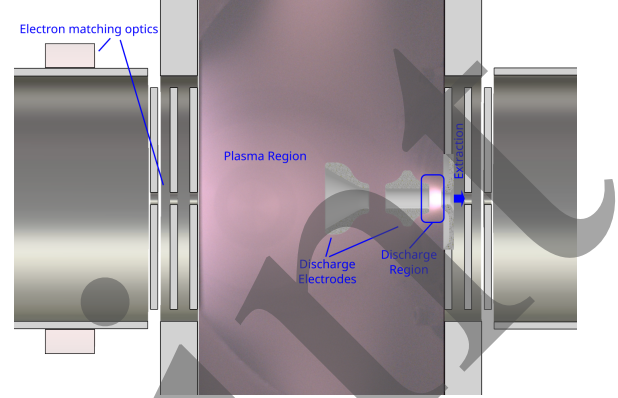


Figure 1: The plasma chamber including hollow discharge electrodes, studied in [1], with the added injection electrodes on the left.

electrodes is the Child-Langmuir law

$$J = \frac{4}{9} \epsilon_0 \sqrt{\frac{2q}{m}} \frac{V^{3/2}}{d^2}, \quad (1)$$

with q the charge and m the mass of the charged particle, V the accelerating voltage and d the distance between the accelerating electrodes. While originally derived for ion discharge currents [6] and later applied to electrons beam formation from a hot cathode surface [7], it is commonly applied to the extraction of ion beams [8,9]. The proportionality of

$$J \propto \frac{V^{3/2}}{d^2} \quad (2)$$

limits the extractable absolute current for a given size of aperture. To overcome this limitation we simulate the effects of a high density electron beam overlapping the ion beam extraction which lowers the local current density due to the opposite charge of the comoving electron beam.

SIMULATION

Setup

The setup of the simulated geometry is based on the plasma generator built for the studies of [1]. It is shown in Fig. 1. The used extraction electrodes used are a simplified triode system used for first tests. To reach the extraction region, the electron beam has to propagate through the plasma generator. To match the electron beam into the plasma region, a similar triode system is used as an injection lens at the opposite of the plasma generator. Additionally for the simulation one solenoid, placed 31 mm before these injection electrodes, is used. A very low energy of 6 keV

* rausch@iap.uni-frankfurt.de

and relatively high current of 100 mA for the electron beam is assumed to both optimize the space charge mitigation but also investigate the electron beam optics at high space charge. A proton beam of 50 mA starts at an assumed optimal plasma sheath surface. The plasma chamber is held at a potential of 22 kV, with the screening electrode at -2 kV. The potential along the axis is shown in Fig. 2. The simulations are performed using CST Studio Suite [10], namely its electro- and magnetostatic solvers as well as its space charge aware particle tracking solver. Three configurations have been investigated, electron beam matching without proton beam, proton beam optics in extraction electrodes without and with electron beam.

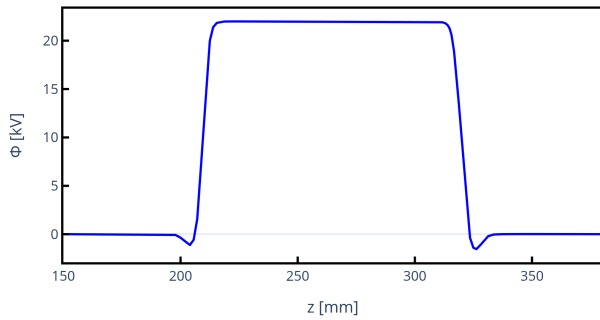


Figure 2: The electric potential Φ on the beam axis z . Inside the plasma region, $\Phi = 22$ kV, in the injection screening electrode on the left it is $\Phi = -1.5$ kV and on the extraction screening electrode $\Phi = -2$ kV

Electron Optics

The setup of the electron optics faces two main challenges. First the beam has to enter the plasma chamber through a relatively small aperture without losses. Second it has to exit the plasma chamber through the extraction aperture well matched to its radius, but also minimizing losses in the following extraction system to avoid sparking in the high voltage gap. While entering the plasma chamber the electron beam is accelerated to the plasma chamber potential, which acts as a strong focusing lens. It has been found that avoiding a strong overfocussing of the beam, it has to be strongly defocused at the entrance of the injection. Therefore the solenoid provides a slight overfocussing before injection, where then the first injection electrode acts additionally as

a defocusing field, before accelerating and focusing into the plasma chamber. With this setting, a roughly parallel beam without losses at injection can be achieved. The simulated trajectories are shown in Fig. 3. The extraction electrodes act on the electron beam in the opposite way. It is decelerated and defocused in the first extraction gap, then focused out of the third electrode. The delicate matching of the beam to this region has shown that there are still losses at the second electrode. This would affect the high voltage extraction gap and can be further optimized by applying additional magnetic focusing or a change of the injection lens geometry to achieve better matching. The simulation of the electron beam tracking has been performed with and without proton beam.

RESULTS

The current density of the simulated proton beam in the extraction potential is shown in Fig. 4 (top). With the compensating electron beam the current density is lowered due to the comoving opposite charge. This is shown in Fig. 4 (bottom). It is also shown that the potential in the extraction region is only slightly deformed by the electron beam, so that apart from mitigating space charge, it does not affect the extraction optics for the proton beam. Figure 5 shows the absolute potential difference in this region when adding the electron beam, which has values smaller than 16 V in the first extraction gap and smaller than 59 V in the second gap. The phase space distribution of the proton beam when the compensating electron beam is present at a position 10 mm after leaving the last aperture is shown in Fig. 6 (top). The distribution of the highly defocused and decelerated electrons is also shown in Fig. 6 (bottom). The phase space distribution of the proton beam is almost unchanged for the non-compensated case. The emittance of the proton beam in both cases is:

$$\text{uncomp. } \varepsilon_{\text{rms}} = 10.93 \text{ mm mrad} \quad (3)$$

$$\text{comp. } \varepsilon_{\text{rms}} = 10.92 \text{ mm mrad} \quad (4)$$

CONCLUSION

It has been shown that an electron beam can be matched to a high potential area of an ion source, where it can propagate through the extraction system. Further optimization

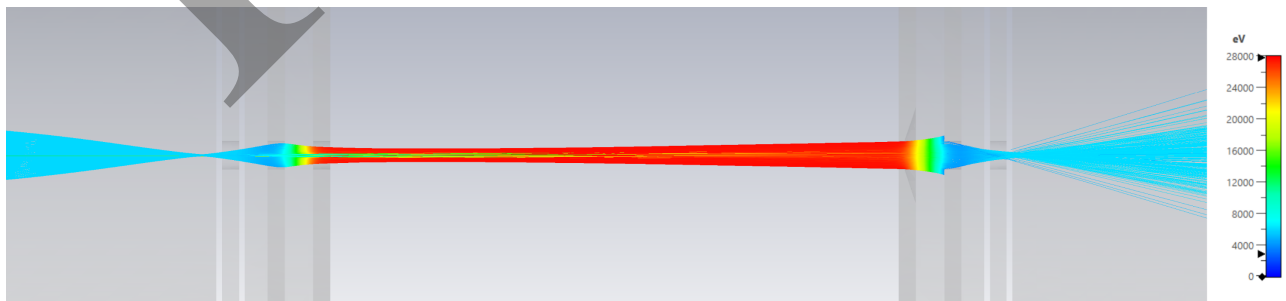


Figure 3: Electron beam trajectories matched to the injection (left) and extraction apertures (right). The colorscale shows the energy of the electrons.

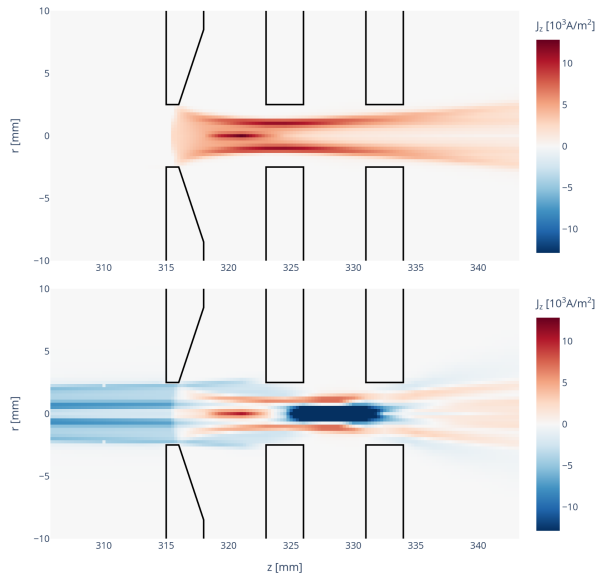


Figure 4: The current density J_z in beam direction in the extraction region for proton beam only (top) and comoving beams (bottom). Note that the colorscale is cut off in the region of large negative current densities to show better the effect in the first extraction gap.

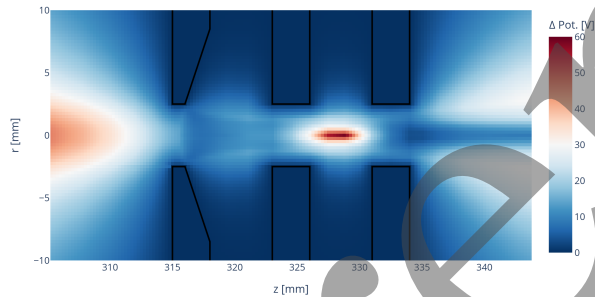


Figure 5: Difference of electric potential in the extraction region between single proton beam and two comoving beams.

is needed to avoid losses at extraction. We found that the current density in the current limiting first extraction gap can be significantly reduced. The deformation of the potential and therefore the electric field in the extraction region by the electron beam is very small relative to the absolute extraction potential difference. The emittances retrieved from the phase space distributions after extraction also confirm, that the effect on the extraction optics is negligible.

OUTLOOK

Further studies of the electron beam matching can improve on mitigating electron losses in the high voltage region. Future investigations using an existing ion source code or even PIC solver to simulate plasma sheath extraction, can clarify how the sheath formation and ion extraction is affected by the electron beam potential. Changed proton beam potential will then also affect the electron beam, so a combined

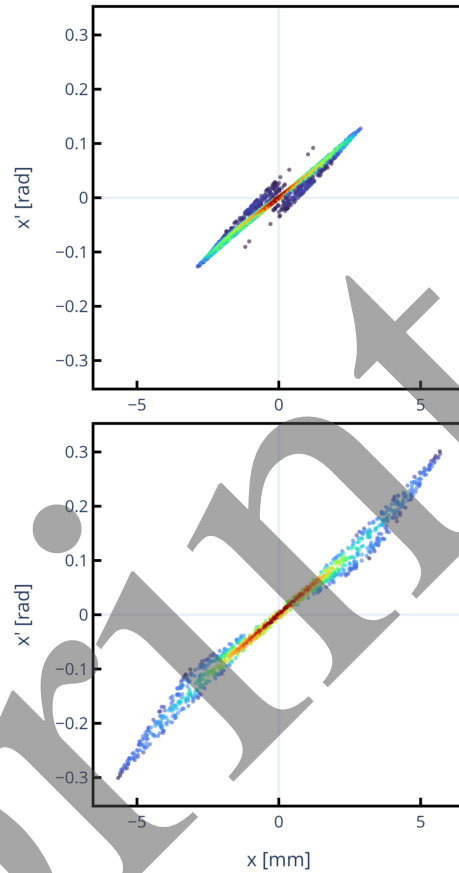


Figure 6: The phase space distributions of comoving protons (top) and electrons (bottom) at a position $z = 344$ mm, 10 mm downstream of the last aperture.

two beam optics optimization should be performed. An experimental setup to validate the findings from simulation is being prepared.

REFERENCES

- [1] J. Rausch *et al.*, “Hybrid plasma generator for high intensity fast pulsed ion sources”, in *Proc. IPAC’24*, Nashville, TN, May 2024, pp. 2694–2697. [doi:10.18429/JACoW-IPAC2024-WEPS03](https://doi.org/10.18429/JACoW-IPAC2024-WEPS03)
- [2] P. Spiller *et al.*, “Approaches to high intensities for FAIR”, in *Proc. 10th European Particle Accelerator Conference (EPAC’06)*, Edinburgh, Scotland, Jun. 2006, pp. 24–28, 2006. proceedings.jacow.org/e06/PAPERS/MOZAPA01.pdf
- [3] H. Podlech *et al.*, “Conceptual Design of the Proton LINAC for the High Brilliance Neutron Source HBS”, in *Proc. IPAC’19*, Melbourne, Australia, May 2019, pp. 910–913. [doi:10.18429/JACoW-IPAC2019-MOPTS027](https://doi.org/10.18429/JACoW-IPAC2019-MOPTS027)
- [4] “The High-Luminosity LHC Project”, Rep. CERN/SPC/1068, CERN/FC/6014, CERN/3255, 2016. <https://cds.cern.ch/record/2199189>
- [5] U. Herleb, “Neutralisation der Raumladung eines Aluminiumionenstrahls mit gepulsten Elektronenstrahlen”, Ph.D. thesis, Universität Erlangen-Nürnberg, Nürnberg, Germany, 1997.

- [6] C. D. Child, “Discharge from hot CaO”, *Phys. Rev. (Series I)*, vol. 32, no. 5, pp. 492–511, May 1911.
[doi:10.1103/PhysRevSeriesI.32.492](https://doi.org/10.1103/PhysRevSeriesI.32.492)
- [7] I. Langmuir, “The Effect of Space Charge and Residual Gases on Thermionic Currents in High Vacuum”, Dec. 1913,
[doi:10.1103/physrev.2.450](https://doi.org/10.1103/physrev.2.450),
- [8] R. Scrivens, “Electron and ion sources for particle accelerators”, in *CAS: Intermediate Course on Accelerator Physics*,
D. Brandt, Ed. 2006. [doi:10.5170/CERN-2006-002.495](https://doi.org/10.5170/CERN-2006-002.495)
- [9] I. Brown, “Vacuum Arc Ion Sources”, in *CAS, Ion Sources*,
R. Bailey, Ed. 2013, pp. 311–329.
[doi:10.5170/CERN-2013-007.311](https://doi.org/10.5170/CERN-2013-007.311)
- [10] Dassault Systèmes, CST Studio Suite, 2024, <https://www.3ds.com/products/simulia/cst-studio-suite>

Preprint